INTERFEROMETRIC SYNTHETIC APERTURE RADAR STUDIES OF ALASKA VOLCANOES

Zhong Lu and **Timothy Masterlark**
U.S. Geological Survey (USGS)
EROS Data Center, Raytheon ITSS
47914 252nd Street
Sioux Falls, SD 57198
lu@usgs.gov, masterlark@usgs.gov

Charles Wicks, Jr. and **Wayne Thatcher**
USGS, Earthquake & Volcano Hazards Program
345 Middlefield Rd.
Menlo Park, CA 94025
cwicks@usgs.gov, thatcher@usgs.gov

Daniel Dzurisin
USGS, Cascades Volcano Observatory
1300 S.E. Cardinal Court, Suite 100
Vancouver, WA 98683-9589
dzurisin@usgs.gov

John Power
USGS, Alaska Volcano Observatory
4200 University drive
Anchorage, AK 99508
jpower@usgs.gov

ABSTRACT

Interferometric synthetic aperture radar (InSAR) imaging is a recently developed geodetic technique capable of measuring ground-surface deformation with centimeter to subcentimeter vertical precision and spatial resolution of tens-of-meters over a relatively large region (~10^4 km^2). This paper summarizes our recent InSAR studies of several Alaska volcanoes including New Trident, Okmok, Akutan, Kiska, Augustine, Westdahl, Peulik, Shishaldin, and Seguam. The spatial distribution of surface deformation data, derived from InSAR images, enables the construction of detailed mechanical models to enhance the study of magmatic and tectonic processes. These studies will improve our understanding on how the Aleutian volcanoes work and our capability to predict future eruptions and the associated hazards.

INTRODUCTION

The Aleutian Arc contains roughly ten percent of the world's active volcanoes. Hardly a year goes by without a major eruption from a volcano in the Aleutian Arc, and more than 170 eruptions were recorded in this area during the last 100 years. The exposure of human life and enterprise to volcano hazards continues to increase because of the expanding national and international air traffic over the Aleutian arc the population increase.

Study of Alaska volcanoes using interferometric synthetic aperture radar (InSAR) has been motivated by two primary factors. First, many volcanic eruptions are preceded by pronounced ground deformation in response to increasing pressure from magma chambers, or to the upward intrusion of magma (Dvorak and Dzurisn, 1997; Dzurisin, 2002). In general, it is expected that a volcano is subject to inflation prior to an eruption, in which case magma migrates from depth, causing localized inflation. Subsequent eruption causes deflation as some or all of this magma is erupted to the surface. Analysis of surface deformation associated with eruptions or intrusions, along with seismicity and other information, provide significant inputs for studying magma dynamics. Second, although the rate of eruptive activities in the arc is very high, these volcanoes remain relatively poorly studied due to the remote

locations, difficult logistics, high cost of field measurement, and persistent cloud cover. Therefore InSAR can significantly improve our understanding of activity at these volcanoes, and enhance our capability to predict future eruptions and mitigate the associated hazards.

We study magma body systems by mapping the surface deformation and modeling the observed deformation. The deformation is measured using the InSAR technique (Massonnet and Feigl, 1998; Rosen et al., 2000) with images collected by ERS-1/ERS-2 satellites. InSAR measures the corresponding phase difference resulting from the difference in the round trip path length to the same ground point between two synthetic aperture radar (SAR) images. The phase difference is due mainly to five effects: (1) differences in the satellite orbits in the two passes, (2) topography, (3) ground deformation, (4) atmospheric propagation delays, (5) systematic and environmental noise. Knowledge of the position and attitude of satellites is required to remove the effect caused by the differences in the satellite orbits of the two passes. The topographic effects in the interferogram can be removed by producing a synthetic interferogram based on an accurate digital elevation model (DEM) and subtracting it from the interferogram to be studied (Massonnet and Feigl, 1998; Rosen et al., 2000). This results in a deformation interferogram. The component of ground deformation along the satellite's look direction can potentially be measured with a precision of from sub-centimeters to centimeters using C-band ERS-1/ERS-2 SARs. Because of problematic atmospheric propagation delays, repeat observations are important to confidently interpret small geophysical signals related to volcanic activities (Zebker et al., 1997; Lu et al., 2000a). To understand the magma processes, we use numerical models to estimate physical parameters based on the observed deformation (Mogi, 1958; Okada, 1985). These models provide insightful evidence of magma processes.

In this paper, we summarize our recent InSAR studies at six Alaska volcanoes, including New Trident, Okmok, Akutan, Kiska, Augustine, Westdahl, Peulik, Shishaldin, and Seguam volcanoes (Fig. 1).

INSAR STUDY OF ALASKA VOLCANOES

New Trident Volcano

The first application of InSAR to study surface deformation over the Aleutians was at New Trident volcano. The New Trident volcano (Fig. 1) is one of the five volcanoes of Katmai group. In 1912 Katmai was the site of the largest volcanic eruption in the world during this century centered at Novarupta Dome (Miller et al., 1998). Eruptive activity since 1912 in the Katmai group includes lava flows from the New Trident in 1963. An ERS-1 interferogram indicated about 7-9 cm of uplift from 1993 to 1995 (Lu et al., 1997). Numerical modeling suggested inflation of a magma body located about 2 km beneath the volcano. Shortly thereafter, Alaska Volcano Observatory (AVO) geologists noted signs of dome-like uplift and fumarolic activity at New Trident.

Okmok Volcano

Okmok volcano, a broad shield topped with a 10-km-wide caldera, is located in the central Aleutian arc (Fig. 1). Catastrophic pyroclastic caldera-forming eruptions occurred ~8000 and 2400 years ago (Miller et al., 1998). Eruptions in this century happened in 1931, 1936, 1938, 1943, 1945, 1958, 1960, 1981, 1983, 1986, 1988, and 1997. Intensive InSAR studies were made of the latest eruption of Okmok volcano (February-April 1997) (Lu et al., 1998, 2000a). Interferograms constructed from ERS-1/ERS-2 SAR images indicated surface inflation of more than 18 cm (between 1992 and 1995) prior to eruption in February-April 1997, more than 140 cm of surface deflation associated with the eruption (Fig. 2a), and 5-10 cm/year inflation after the eruption. Numerical modeling suggested the magma reservoir responsible for the eruption resided at about 2~3 km depth beneath the center of the caldera, which was about 5 km from the eruptive vent. This study demonstrated that InSAR is capable of measuring pre-eruptive, co-eruptive, and post-eruptive deformation in the sub-arctic environment (Lu et al., 1998, 2000a).

Akutan Volcano

Akutan is the second most active volcano in Alaska, and sits in the central Aleutian volcanic arc (Fig. 1). In March 1996, an intense swarm of volcano-tectonic earthquakes (~3000 felt by local residents, maximum magnitude 5.1) beneath Akutan Island, produced extensive ground cracks but no eruption of Akutan volcano. InSAR images spanning the time of the swarm revealed complex island-wide deformation: the western part of the island including Akutan volcano moved upward while the eastern part moved downward (Lu et al., 2000c) (Fig. 2b). The axis of the deformation approximately aligns with new ground cracks on the western part of the island and with Holocene normal faults that were reactivated during the swarm on the eastern part of the island. The axis is also roughly parallel to the direction of greatest compressional stress in the region. No ground movements greater than 2.83 cm were observed outside the volcano's summit caldera for periods of 4 years before the swarm (Lu et al., 2000c). With

the observed deformation, seismicity, and ground cracks as input, we modeled the deformation primarily as the emplacement of a shallow, east-west-trending, north-dipping dike plus inflation of a deep Mogi-type magma body beneath the volcano. The pattern of subsidence on the eastern part of the island is poorly constrained. It might have been produced by extensional tectonic strain that both reactivated preexisting faults on the eastern part of the island and facilitated magma movement beneath the western part. Alternatively, magma intrusion beneath the volcano may have been the cause of extension and subsidence in the eastern part of the island. This study demonstrated that InSAR can not only provide a basis for interpreting and modeling movement of shallow magma bodies that feed eruptions, but also for detecting intrusive activities that do not result in an eruption (Lu et al., 2000c).

Kiska Volcano

Kiska volcano is the westernmost historically active volcano in the Aleutian arc, Alaska (Fig. 1). Sequential interferometric synthetic aperture radar images of Kiska, the westernmost historically active volcano in the Aleutian arc, show that a circular area about 3 km in diameter centered near the summit subsided by as much as 10 cm from 1995 to 2001, mostly during 1999 and 2000 (Lu et al., 2002b) (Fig. 2c). An elastic Mogi-type (Mogi, 1958) deformation model suggests that the source is within 1 km of the surface. Based on the shallow source depth, the copious amounts of steam during recent eruptions, and recent field reports of vigorous steaming and persistent ground shaking near the summit area, we attribute the subsidence to decreased pore-fluid pressure within a shallow hydrothermal system beneath the summit area (Lu et al., 2002b).

Augustine Volcano

Augustine volcano, an 8 by 11 km island, is located in lower Cook Inlet, Alaska (Fig. 1). The volcano consists of a central dome and lava flow complex, surrounded by pyroclastic debris (Miller et al., 1998). Augustine volcano has had six significant eruptions in last two centuries: 1812, 1883, 1935, 1963-64, 1976, and 1986. Eruptions typically consist of multiple phases spanning several months; explosive ash eruptions are often accompanied by mud-flows and pyroclastic flows. ERS-1/ERS-2 interferograms showed that the pyroclastic flows from the 1986 eruption have been experiencing subsidence/compaction at a rate of about 3 cm per year (Fig. 2d). The observed deformation will be used to study the characteristics of the pyroclastic flows. No sign of significant volcano-wide deformation has been observed since 1992.

Westdahl Volcano

Westdahl is a young glacier-clad shield volcano located on the central Aleutian arc (Fig. 1). The edifice is composed of a thick sequence of pre-glacial basalt lava flows. The volcano was frequently active during the latter half of the 20^{th} century, with documented eruptions in 1964, 1978-79, and 1991-92 (Miller al., 1998). The background level of seismic activity since the last eruption in 1991-92 has been low (about five $M < 3$ earthquakes per year) and no unusual activity has been detected. Using ERS-1/ERS-2 interferograms, we mapped the progressive inflation of Westdahl volcano, Alaska, during a six-year period of quiescence following its most recent eruption in 1991-92 (Lu et al., 2000b). About 17 cm of volcano-wide inflation from September 1993 to October 1998 was observed (Fig. 2e). Multiple independent interferograms reveal that inflation rate decreases with time during 1992 and 2000. The rates of inflation is approximated by exponential decay functions with time constant of about 6 years. Such a behavior is consistent with a deep, constant-pressure magma source connected to a shallow reservoir via a conduit. This example demonstrates that InSAR seems to be the best tool available for detecting deep, aseismic magma accumulation by measuring broad, subtle deformation of the ground surface, to identify restless volcanoes long before they become active, and before seismic and other precursors emerge (Lu et al., 2000b).

Peulik Volcano

Peulik, a stratovolcano, is located on the Alaska Peninsula about 550 km southwest of Anchorage, Alaska (Fig. 1). The volcano has been active only twice during historical time, in 1814 and 1852, and was otherwise quiescent during the 1990s (Miller et al., 1998). A series of ERS interferograms that collectively span the time interval from July 1992 to August 2000 reveal that a presumed magma body located 6.6 ± 0.5 km beneath the Peulik volcano inflated 0.051 ± 0.005 km^3 between October 1996 and September 1998 (Lu et al., 2002a). The average inflation rate of the magma body was about 0.003 km^3/month from October 1996 to September 1997 (Fig. 2f), peaked at 0.005 km^3/month during June 26-October 9, 1997, and dropped to 0.001 km^3/month from October 1997 to September 1998. Deformation before October 1996 or after September 1998 is not significant (Lu et al., 2002a). An intense earthquake swarm, occurred about 30 km northwest of Peulik from May to October, 1998, around the end of the inflation period. The 1996-98 inflation episode at Peulik confirms that InSAR can be used to detect magma

accumulation beneath dormant volcanoes at least several months before other signs of unrest are apparent. This application represents a first step toward understanding the eruption cycle at Peulik and other stratovolcanoes with characteristically long repose periods (Lu et al., 2002a).

Shishaldin Volcano

Shishaldin volcano (Fig. 1) is located near the center of Unimak Island in the eastern Aleutians. The spectacular symmetric cone has a base diameter of approximately 10 miles (16 km) and a small summit crater that typically emits a steam plume with occasional small amounts of ash. Shishaldin volcano is the third most active volcano in the Aleutian arc, having erupted at least 28 times since 1775 and most recently in May 1999 (Miller et al., 1998). Fig. 3 shows two interferograms from two adjacent tracks. The interferogram on the left (Fig. 3) spanned the summers of 1997 and 1999, while the images used for the interferogram on the right (Fig. 3) were acquired in summers of 1998 and 1999. Shishaldin is the tallest volcano in the Aleutians. The summit area (~5 km radius) is covered by snow and ice most of the year, and therefore does not maintain coherence for C-band ERS interferograms. No significant deformation was observed in the coherence areas. We also produced several interferograms several years before the eruption and several years after the eruption, no significant amount of deformation was observed for either time interval. This suggested three possible scenarios: 1) no significant pre-eruptive and co-eruptive deformation was associated with the 1999 eruption; 2) pre-eruptive inflation was balanced by co-eruptive deflation and no net displacement could be observed; 3) the magma source is very shallow and magma strength is small so that deformation could only occur over the region of lost coherence. Viewing the size of the May 1999 eruption, and the last interpretation is the least likely one of the three.

Seguam Volcano

Seguam Island (Fig. 1) consists of two late Quaternary calderas (Fig. 4a). The western caldera, Pyre Peak (commonly referred to as Seguam volcano), dominates the western half the island. Pyre Peak is about 3 km wide, has a central cone, and is the source of most of the historical eruptions over the island. The eastern caldera also has a central cone. Historical eruptions in this century occurred in 1901, 1927, and 1977. In later December 1992, Pyre Peak erupted with an ash cloud rising up to 1200 m. Explosive eruptions were reported from May 28 to August 19, 1993. Figures 4b-4d show interferograms that span three different time intervals. Ground surface deformation during January and August, 1993, which brackets several eruptions from May to August 1993, is shown in Fig. 4b. Even though the eruptions happened at the Pyre Peak, our preliminary results indicate the western part of the island did not move much while the eastern caldera inflated about 3 cm. From June 1993 to September 1995, the southern flank of Pyre Peak subsided about 3 cm while the eastern caldera subsided more than 4 cm (Fig. 4c). From July 1999 to October 2000, most of the deformation occurred over the eastern caldera, which inflated nearly 5 cm (Fig. 4d). Detailed analysis and modeling of the dynamic deformation of Seguam Island is currently being conducted.

SUGGESTIONS & CONCLUSIONS

The evolving satellite radar imagery combined with InSAR techniques has proven a powerful space geodetic tool to study volcanic eruptions, detect aseismic deformation at quiescent volcanoes preceding seismic swarms, enhance our understanding of volcanic plumbing systems, and guide scientists to better focus their monitoring and hazards mitigation efforts. However, the range change caused by the atmospheric delays is significant for interferograms over the Aleutian volcanoes. For example, a range change up to 6 cm was detected over a distance of 8 km over Okmok volcano (Lu et al., 2000a). Therefore, multiple observations from independent interferograms for similar time intervals should be used to verify any apparent deformation (Zebker et al., 1997; Lu et al., 2000a). Also, reduction of radar coherence is the major obstacle to applying InSAR on Aleutian volcanoes. At Alaska volcanoes, processes that reduce interferometric coherence include snow/ice melting and accumulation, freezing/thawing of surface material, erosion/deposition of volcanic ash, and dense vegetation. Therefore, the best chance of producing coherent interferograms is to use images acquired during summer or early fall, separated in time by one to a few years (Lu and Freymueller, 1998). Nevertheless, good coherence at C-band can be maintained for at least three to five years on some volcanic surfaces. To obtain the most usable results for reliably near-real time monitoring of restless volcanoes in sub-arctic environment, future C-band satellite passes must be made at least every month from July through September, every week during the late spring/early summer or late fall, and every 2-3 days during the winter (Lu and Freymueller, 1998). The spatial baseline length should be as small as possible to reduce the decorrelation effects.

ACKNOWLEDGMENT

ERS-1/ERS-2 SAR images are copyright © 1992-2001 ESA. The research summarized in the paper were supported by funding from NASA Radarsat Program and Solid Earth & Natural Hazards Program, USGS contract 1434-CR-97-CN-40274, and USGS Volcano Hazard Program. We thank the Alaska SAR Facility (ASF) for their special efforts in making the SAR data available, NASA/JPL for providing SRTM DEM, J. Freymueller, C. Werner, S. Moran, D. Mann, D. Meyer, and S. McNutt for contributions to this research.

References

Dvorak, J., and D. Dzurisin (1997). Volcano geodesy: The search for magma reservoirs and the formation of eruptive vents, *Rev. Geophys.*, 35:343-384.

Dzurisin, D. (2002). A comprehensive approach to monitoring volcano deformation as a window on eruption cycle, *Rev. Geophys*., in press.

Lu, Z., R. Fatland, M. Wyss, S. Li, J. Eichelberger, K. Dean, and J. Freymueller (1997). Deformation of New Trident volcano measured by ERS-1 SAR interferometry, Katmai national Park, Alaska, *Geophys. Res. Lett.*, 24:695-698.

Lu, Z., D. Mann, and J. Freymueller (1998). Satellite radar interferometry measures deformation at Okmok Volcano, *Eos Trans*., 79:461-468.

Lu, Z., and J. Freymueller (1998). Synthetic aperture radar interferometry coherence analysis over Katmai volcano group, Alaska, *J. Geophys. Res*., 103:29,887-29,894.

Lu, Z., D. Mann, J. Freymueller, and D. Meyer (2000a). Synthetic aperture radar interferometry of Okmok volcano, Alaska 1: Radar observations, *J. Geophys. Res*., 105:10791-10806.

Lu, Z., C. Wicks, D. Dzurisin, W. Thatcher, J. Freymueller, S. McNutt, and D. Mann (2000b). Aseismic inflation of Westdahl volcano, Alaska, revealed by satellite radar interferometry, *Geophys. Res. Lett.*, 27:1567-1570.

Lu, Z., C. Wicks, J. Power, and D. Dzurisin (2000c). Deformation of Akutan volcano, Alaska, revealed by satellite radar interferometry, *J. Geophys. Res.*, 105:21483-21496.

Lu, Z., C. Wicks, D. Dzurisin, J. Power, S. Moran, and W. Thatcher (2002a), Magmatic inflation at a dormant stratovolcano: 1996-98 activity at Mount Peulik volcano, Alaska, revealed by satellite radar interferometry, *J. Geophys. Res*., 107:10.1029/2001JB0009471.

Lu, Z., T. Masterlark, J. Power, D. Dzurisin, and C. Wicks (2002b), Summit subsidence at Kiska volcano, western Aleutians, detected by satellite radar interferometry, *Geophys. Res. Lett.*, 29:10.1029/2002GL01498.

Massonnet, D., and K. Feigl (1998). Radar interferometry and its application to changes in the Earth's surface, *Rev. Geophys.*, 36:441-500.

Miller, T.M., and others (1998). Catalog of the historically active volcanoes of Alaska, *USGS Open-File Report*, 98-582.

Mogi, K. (1958). Relations between the eruptions of various volcanoes and the deformations of the ground surface around them, *Bull. Earthquake Res. Inst. Univ. Tokyo*, 36:99-134.

Okada, Y. (1985). Surface deformation to shear and tensile fault in an elastic half-space, *Bull. Seismol. Soc. Am.*, 75:1135-1154.

Rosen, P. and others (2000). Synthetic aperture radar interferometry, *Proceedings IEEE*, 88:333-380.

Zebker, H., P. Rosen, and S. Hensley (1997). Atmospheric effects in interferometric synthetic aperture radar surface deformation and topographic maps, *J. Geophys. Res.*, 102:7547-7563.

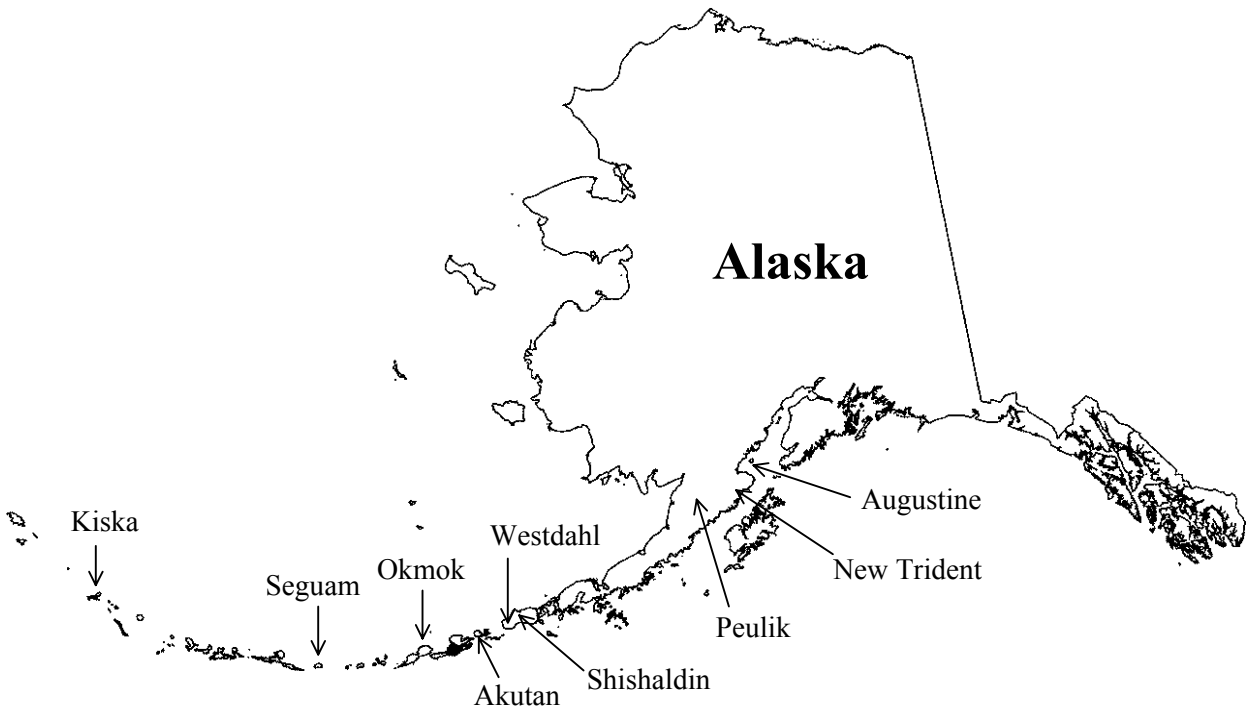

Fig. 1. Location map showing the Alaska volcanoes reported in this paper.

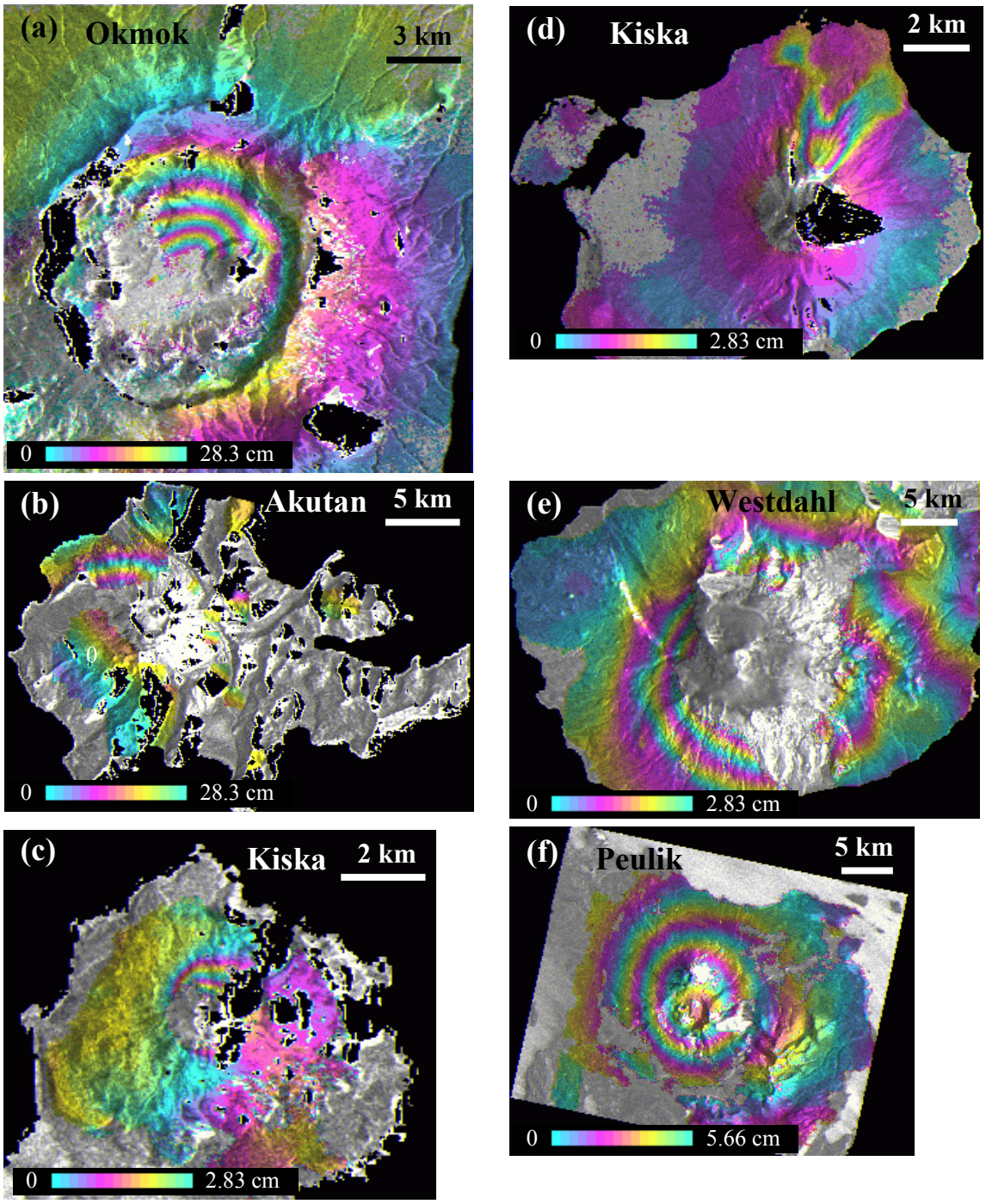

Fig. 2. (a) Deformation interferogram (Oct. 1995 – Sep. 1997), bracketing the Feb. – Apr. 1997 eruption of Okmok volcano. (b) Deformation interferogram of Akutan volcano, spanning the March 1996 seismic swarm. (c) Deformation interferogram for Kiska volcano during Aug. 1999 and Aug. 2000. (d) Interferogram of Augustine volcano (1992-1993), depicting the deformation associated with the compaction of the 1986 pyroclastic flow deposits. (e) Aseismic inflation of Westdahl volcano, observed from a 1993-1998 InSAR image. (f) Interferogram (Oct. 1996 – Oct. 1997), representing ~17 cm of uplift centered on the southwest flank of Peulik volcano. Dark regions indicate areas with severe geometric distortion in the SAR images due to the side-looking nature of the radar sensor. Areas without interferometric coherence are uncolored.

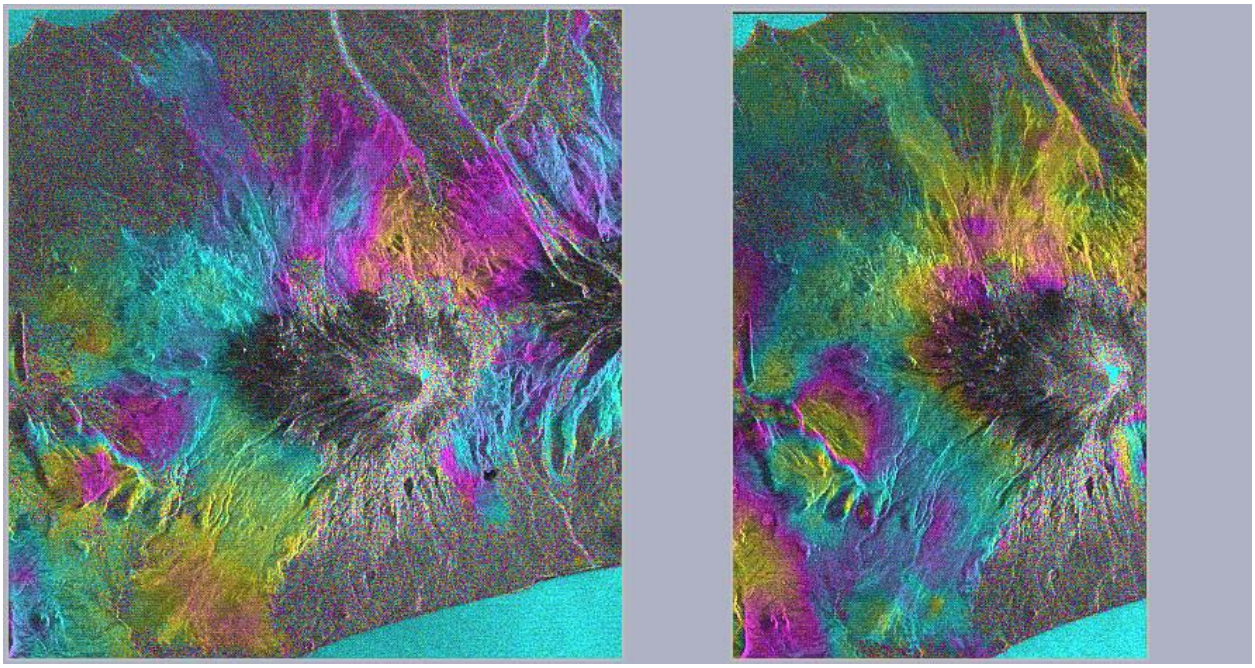

Fig. 3. Topography-removed interferograms spanning the May 1999 eruption of Shishaldin volcano.

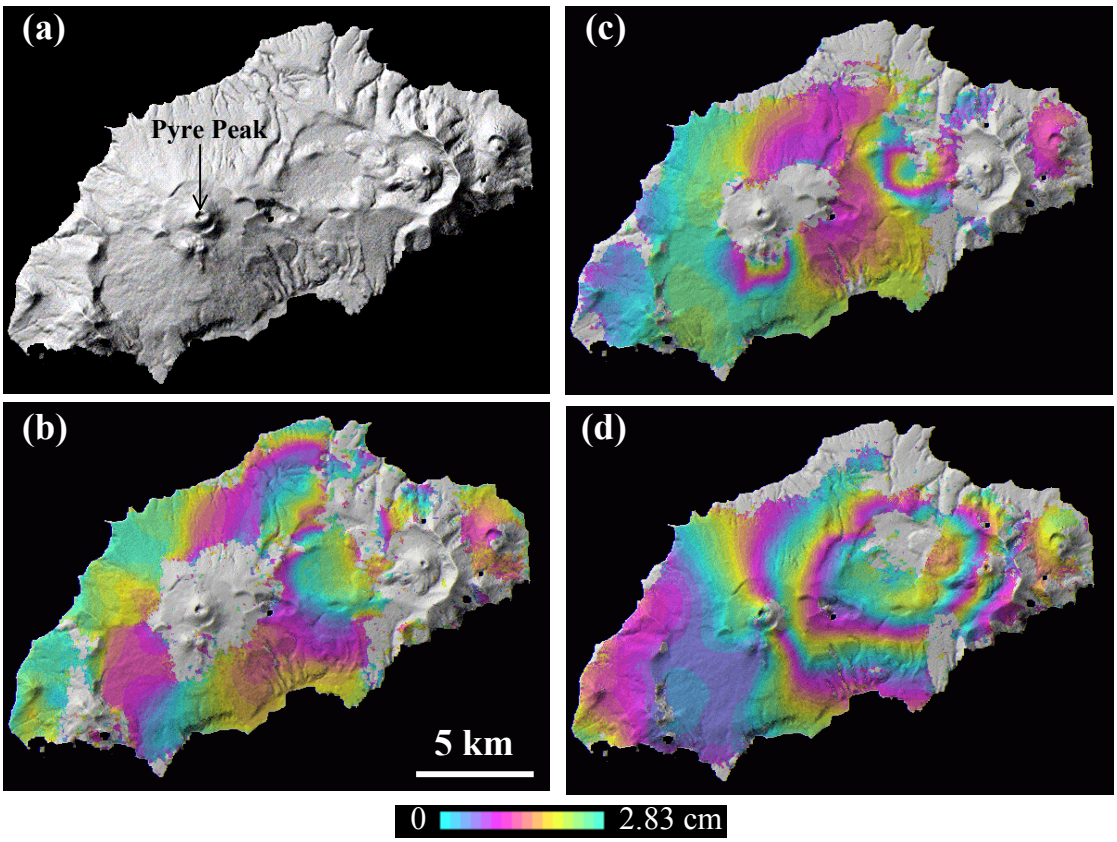

Fig. 4. (a) Shaded-relief map of Seguam produced from the SRTM DEM. Deformation interferograms are for the periods (b) January to August 1993, (c) June 1993 to September 1995, and (d) July 1999 to September 2000. Each interferometric fringe (full color cycle) represents 2.83 cm of range change between the ground and the satellite. Areas without interferometric coherence are uncolored.